Highly charged cellulose nanocrystals as flocculants for algal biomass – Supporting Information

Dries Vandamme, Samuel Eyley, Guy Van den Mooter,

Koenraad Muylaert, Wim Thielemans*

wim.thielemans@kuleuven-kulak.be

July 29, 2015

Contents

List of Figures

List of Tables

S1 Synthetic details

S1.1 Chemical characterization

Infrared spectra were recorded on a Bruker Alpha FTIR spectrometer in ATR mode. Data were recorded between $4000 - 400\,\mathrm{cm^{-1}}$ over 16 scans with $4\,\mathrm{cm^{-1}}$ resolution. The resulting peaks for cellulose were assigned using data from [1] on the assignment of the FTIR spectrum for Cellulose I_β.

ζ-potential titration was performed by suspending 50 mg of each sample in 50 mL deionized water followed by addition of sodium carbonate solution (1 M) until the resulting pH was between $10 - 11$. The suspension was then sonicated for 5 min prior to starting of the ζ-potential measurements. ζ-potential measurements were carried out on a Brookhaven Instruments NanoBrook Omni in phase analysis light scattering (PALS) mode. Equilibration for 5 min was allowed before collection and ζ-potential was averaged over five measurements of 30 cycles each. pH was adjusted using hydrochloric acid (1 M) between sets of measurements.

Dye adsorption experiments were performed by suspending $0 - 2$ mg CNCs in orange II solution (50 µM, 20 mL) and agitating for 5 min before filtering through a 0.2 µm glass microfibre/cellulose acetate syringe filter. The UV-vis spectrum of the resulting dye solution was measured on a Shimadzu UV-1800 spectrophotometer in quartz cells with a 1 cm path length. Dye adsorption was calculated from the loss in absorbance of the dye solution at 484 nm after mixing with CNCs. The response of the spectrophotometer was calibrated using 11 concentrations of orange II between $1.3 \times 10^{-6} - 5 \times 10^{-5}$ M and the molar extinction coefficient calculated as $19\,855\,\mathrm{M^{-1}\,cm^{-1}}$ (calibration curve in supporting information).

Elemental analysis (C, H, N, S) data were collected on a Thermo Flash 2000 elemental analyzer using methionine as a calibration standard with linear calibration (0.3 % accuracy). Halide elemental analysis data (Cl, Br) were collected by Service Central d'Analyse - Institut des Sciences Analytiques in Lyon, France (0.2 % accuracy). Degree of substitution (DS) was calculated using an iterative procedure whereby the empirical formula of the graft added to cellulose was added to the empirical formula of the anhydroglucose unit until the percentage of nitrogen was equal in the calculated elemental analysis results and the actual results. Nitrogen was chosen due to the absence of this element in the starting material and importance in the subsequent use of the material as a flocculant. Water content of each of the samples was determined by thermogravimetric analysis (TGA) performed on a TA instruments AutoTGA 2950HR under nitrogen. Samples were heated at 10 °C min^{-1} to 120 °C, followed by an isothermal period for 1 h, then continued heating at 10 °C min^{-1} to 600 °C. Water content was determined as mass loss at 125 °C.

X-ray diffraction data were collected on a PANalytical X'Pert Pro multi-purpose diffractometer (MPD) in Bragg-Brentano parafocusing geometry, with Cu K_α (45 kV, 40 mA) radiation, automated divergence and receiving slits (10 mm illuminated length), 10 mm beam mask and a step size of 0.02°. Samples were analyzed on a silicon "zero-background" sample holder as a loose powder with the packing density influencing the amount of sample in the beam (freeze-dried samples are less aggregated). The sample stage was rotated during acquisition to reduce preferred orientation effects in the plane of the stage. The empty sample holder was scanned and used as an instrumental background. The acquired instrumental background data were subtracted before further analysis. Profex with the BGMN backend was used to perform fitting of the cellulose Iβ pattern from [2] to the experimental data using a Rietveld refinement algorithm. The data was fitted between 10 – 40° 2θ using a polynomial background function, anisotropic size broadening, isotropic strain broadening and anisotropic preferred orientation functions. For the resulting fitted data, the crystallinity index (χ_c) of the cellulose was calculated as described by [3] using equation (2) where s is the scattering vector described by equation (1), $I_c(s)$ is the intensity at a particular vector due to crystalline material and $I(s)$

is the total intensity at a particular vector. The limits of the integration were chosen so that s_0 is the scattering vector at $2\theta = 10°$ ($0.23\,\text{Å}^{-1}$) and s_1 is the scattering vector at $2\theta = 40°$ ($0.83\,\text{Å}^{-1}$).

$$s = \frac{2\sin\theta}{\lambda} \tag{1}$$

$$\chi_c = \frac{\int_{s_0}^{s_1} I_c(s)s^2 ds}{\int_{s_0}^{s_1} I(s)s^2 ds} \tag{2}$$

X-ray photoelectron spectroscopy data were collected at Thermo Fisher Scientific applications laboratory (East Grinstead) on an ESCAlab 250Xi spectrometer with monochromated Al K_α (1486 eV) radiation. The X-ray gun was operated with a 650 µm spot size (200 W) and spectra were collected under charge neutralization conditions (dual source co-axial electron and external Ar^+/e^- flood gun). The lens was operated in magnetic mode, and the hemisphere analyzer in Constant Analyzer Energy (CAE) mode, with electron detection using a six channel electron multiplier. The pass energy for survey scans was 200 eV and for high resolution scans was 12, 20 or 50 eV depending on sample conditions. The resulting spectra were processed using CasaXPS software. Binding energy was referenced to adventitious carbon at 285 eV. High resolution spectra were fitted with Voigt type peaks with some asymmetry correction based on the vibrational modes of the cellulose molecule, which cause peak broadening due to some photon energy being absorbed by vibrational transitions in the bonds connected to the atom of interest [4, 5]. This results in small peaks at higher binding energy associated with the main photoelectron line. The separation of these peaks from the main peak are determined by the energy of the vibrational transition. By considering the FTIR spectrum of the compound and converting the energy of the vibrational modes to electron volts, the asymmetry was set for each component peak in the high resolution spectrum, based on the vibrational modes present in the bonds connected to that atom [5].

S1.2 Synthesis of cellulose nanocrystals (CNCs)

Sulfuric acid (550 mL, 10.06 M) was heated at 45 °C and cotton wool (50 g) added slowly with mechanical stirring. Stirring and heating was continued until 1 h from first addition, before addition of deionized water (800 mL) to quench the reaction. The cellulose was separated from the acidic reaction media by centrifugation (20 000 × g, 10 °C) for 20 min. The solid product was washed with two successive centrifugations (20 000 × g, 10 °C) for 35 min, before dialyzing against running deionized water for 48 h in a regenerated cellulose dialysis tube (MWCO 12 – 14 kDa). The nanocrystal suspension was homogenized using a sonication horn before filtration through a porosity 2 fritted glass filter to separate aggregates. The resulting homogeneous suspension was mixed with Amberlite MB 6113 mixed bed ion exchange resin (100 g) for 12 h, separated, frozen in liquid nitrogen, then freeze dried. The cellulose nanocrystals were subsequently Soxhlet extracted with ethanol (48 h) in a cellulose extraction thimble to remove organic surface contaminants and dried in vacuo (14 g, 30 %). Found: C, 43.26; H, 6.05; N, < 0.1; S, < 0.1 %. Calc. for $(C_6H_{10}O_5)_n$ (with 3.34 % adsorbed water): C, 42.96; H, 6.38 %. $\bar{\nu}_{max}$ (ATR) /cm^{-1} 3345 ν(O-H), 2900 ν(C-H), 1644 δ(H_2O), 1428 δ(C-O-H), 1335 δ(C-O-H), 1315 δ(C-O-H), 1205 ν(C-O-C, glycosidic), 1161 ν(C-O-C, glycosidic, asym.), 1109 ν(C2-OH), 1055 ν(C3-OH), 1032 ν(C6-OH), 701 ω(C-OH), 664 ω(C-OH).

S1.3 Synthesis of benzylpyridinium grafted CNCs ([Br][PyBnOO]-g-CNCs)

Cellulose nanocrystals (1 g), 4-(1-bromomethyl)benzoic acid (1.18 g, 5.4 mmol) and *p*-toluenesulfonyl chloride (1.04 g, 5.4 mmol) were suspended in dry pyridine (130 mL) under an argon atmosphere and heated at 80 °C for 14 h before isolation of the solid product by filtration of the suspension through a cellulose Soxhlet extraction thimble. The filtrand was purified by sequential Soxhlet extraction with dichloromethane (24 h) and ethanol (72 h). The resulting nanocrystals were dried in vacuo to yield cream colored solid product. Found: C, 46.90; H, 5.45; N, 1.33; S, 0.39; Cl, 1.16;

Br 4.28 %. Calc. for $C_{8.95}H_{12.29}O_{5.27}N_{0.21}S_{0.03}Br_{0.12}Cl_{0.08}$ (DS = 0.21, 51.6 % bromide, 36.7 % chloride, 11.7 % tosylate counter ion with 2.02 % adsorbed water): C, 47.73; H, 5.72; N, 1.32; S, 0.39; Cl, 1.35; Br, 4.28 %. $\bar{\nu}_{max}$ (ATR) /cm^{-1} 3336 ν(O-H), 2900 ν(C-H), 1717 ν(C=O), 1633 $\delta(H_2O)$/ν(C=C/C=N), 1581 ν(C=C/C=N), 1486 ν(C=C/C=N), 1423 δ(C-O-H), 1336 δ(C-O-H), 1315 δ(C-O-H), 1276 ν(C-O, ester), 1206 ν(C-O-C, glycosidic), 1161 ν(C-O-C, glycosidic, asym.), 1109 ν(C2-OH), 1056 ν(C3-OH), 1032 ν(C6-OH), 755 ω(C-H arom., oop), 705 ω(C-OH), 665 ω(C-OH).

S1.4 Synthesis of α-methylbenzylpyridinium grafted CNCs ([Br][PyMeBnOO]-g-CNCs)

Cellulose nanocrystals (1 g), 4-(1-bromoethyl)benzoic acid (1.24 g, 5.4 mmol) and *p*-toluenesulfonyl chloride (1.04 g, 5.4 mmol) were suspended in dry pyridine (130 mL) under an argon atmosphere and heated at 80 °C for 14 h before isolation of the solid product by filtration of the suspension through a cellulose Soxhlet extraction thimble. The filtrand was purified by sequential Soxhlet extraction with dichloromethane (24 h) and ethanol (72 h). The resulting nanocrystals were dried in vacuo to yield cream colored solid product. Found: C, 49.97; H, 5.36; N, 1.84; S, 0.98; Cl, 1.65; Br 4.95 %. Calc. for $C_{11.97}H_{15.12}O_{5.56}N_{0.38}S_{0.09}Br_{0.18}Cl_{0.17}$ (DS = 0.38, 41 % bromide, 38.5 % chloride, 20.5 % tosylate counter ion with 4.64 % adsorbed water): C, 49.58; H, 5.77; N, 1.84; S, 0.99; Cl, 2.05; Br, 4.95 %. $\bar{\nu}_{max}$ (ATR) /cm^{-1} 3337 ν(O-H), 2901 ν(C-H), 1721 ν(C=O), 1631 $\delta(H_2O)$/ν(C=C/C=N), 1580 ν(C=C/C=N), 1482 ν(C=C/C=N), 1422 δ(C-O-H), 1335 δ(C-O-H), 1316 δ(C-O-H), 1274 ν(C-O, ester), 1205 ν(C-O-C, glycosidic), 1161 ν(C-O-C, glycosidic, asym.), 1109 ν(C2-OH), 1056 ν(C3-OH), 1032 ν(C6-OH), 770 ω(C-H arom., oop), 744 ω(C-H arom., oop), 706 ω(C-OH), 666 ω(C-OH).

S2 FTIR spectra

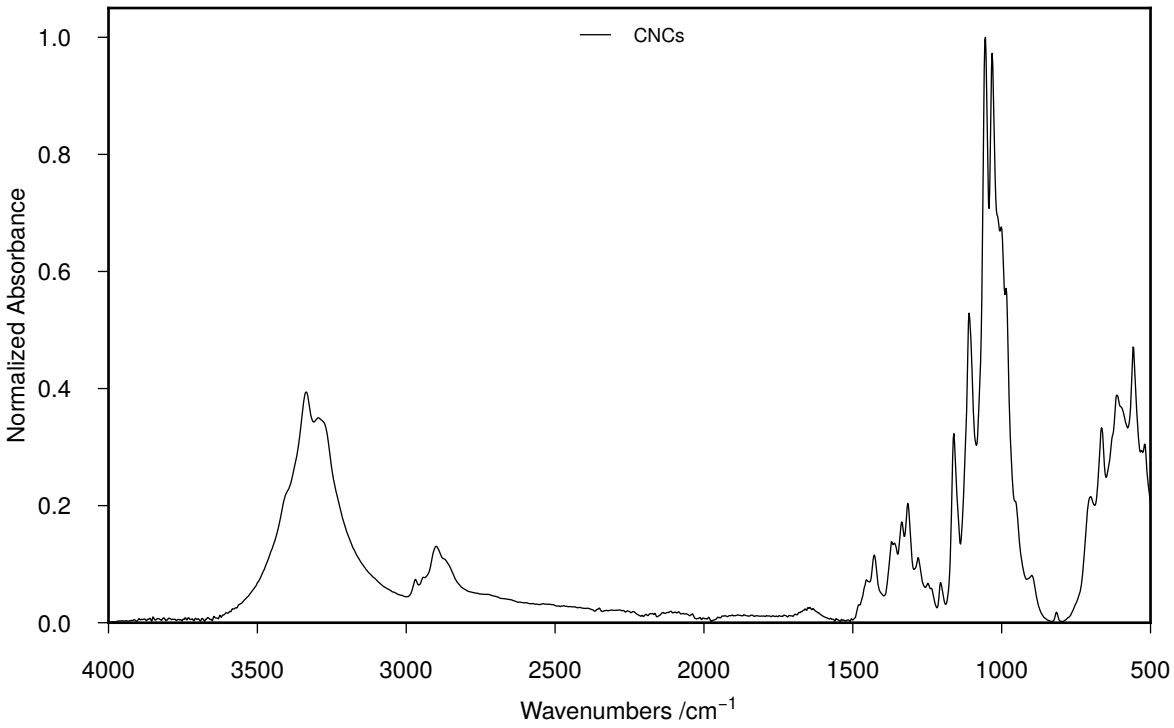

Figure S2.1. FTIR spectrum of unmodified CNCs

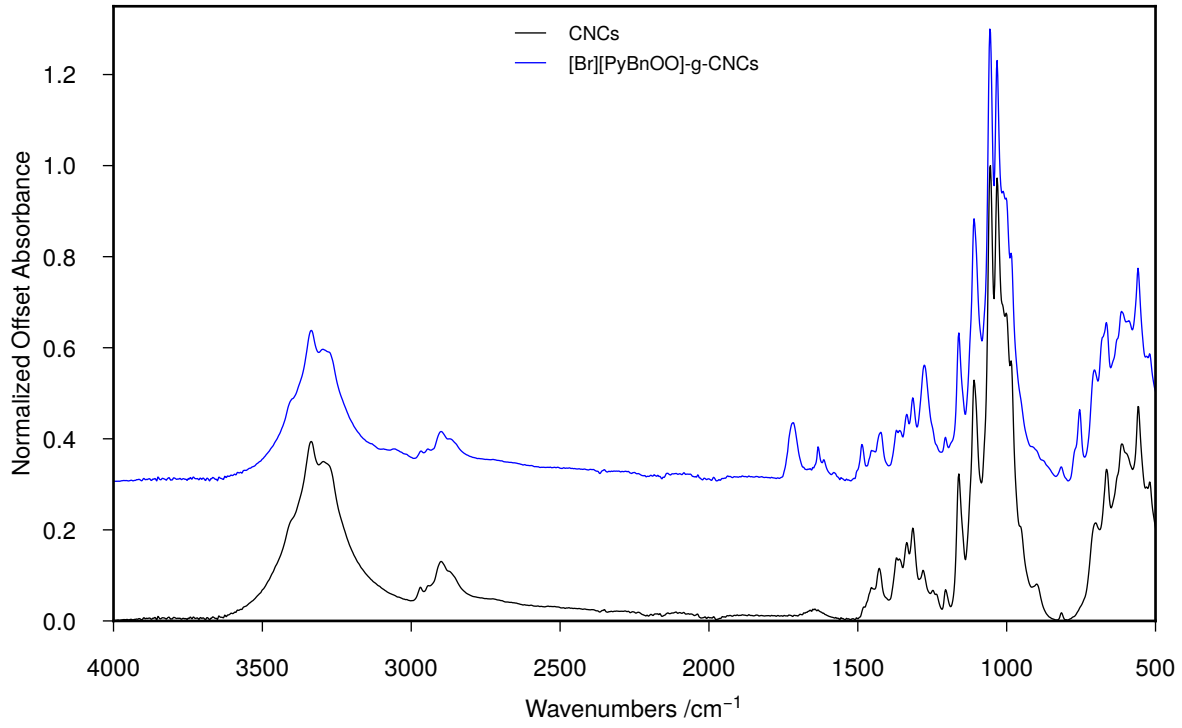

Figure S2.2. FTIR spectrum of [Br][PyBnOO]-g-CNCs

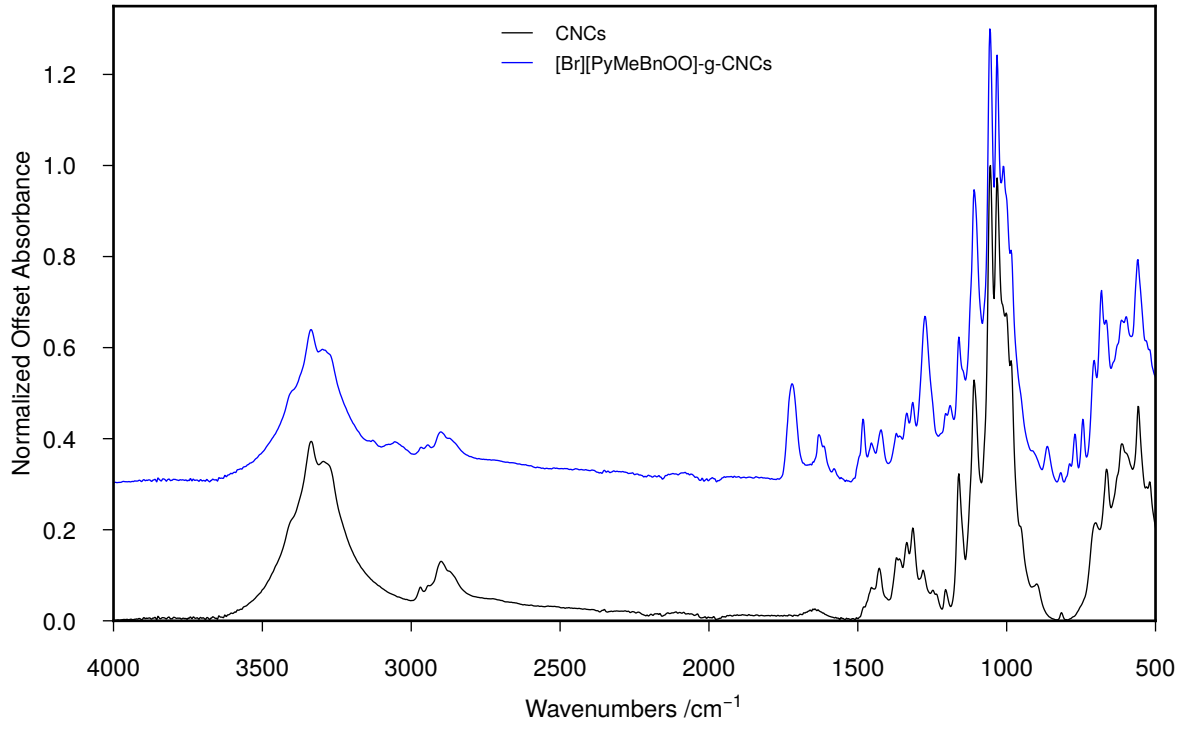

Figure S2.3. FTIR spectrum of [Br][PyMeBnOO]-g-CNCs

S3 Dye adsorption - UVVis spectroscopy

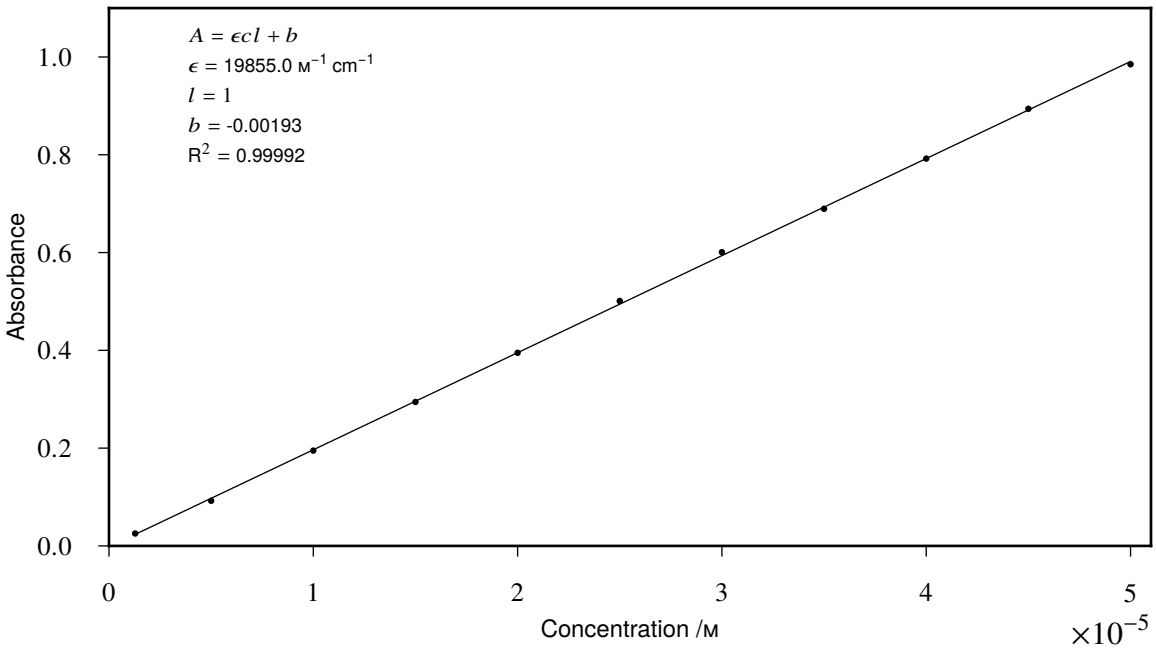

Figure S3.4. Orange II calibration curve

S4 X-ray diffractograms

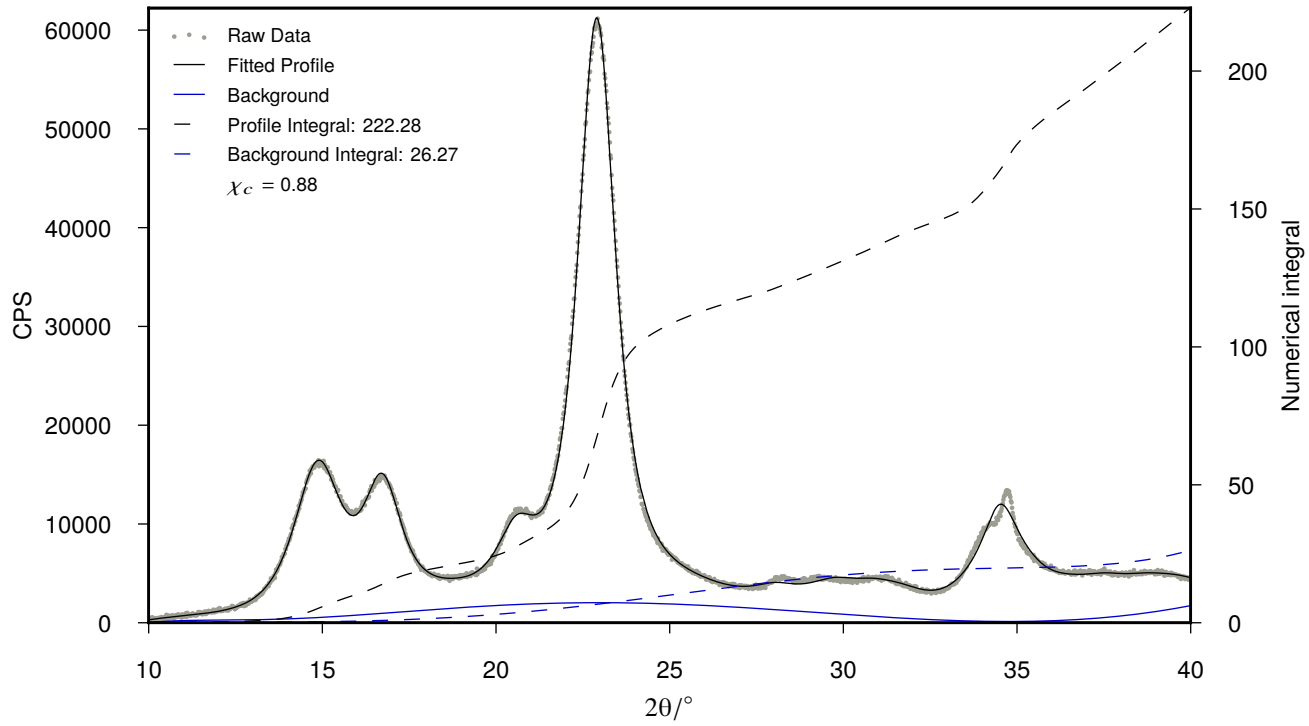

Figure S4.5. XRD of unmodified CNCs showing calculated profile, background, integral curves and crystallinity index

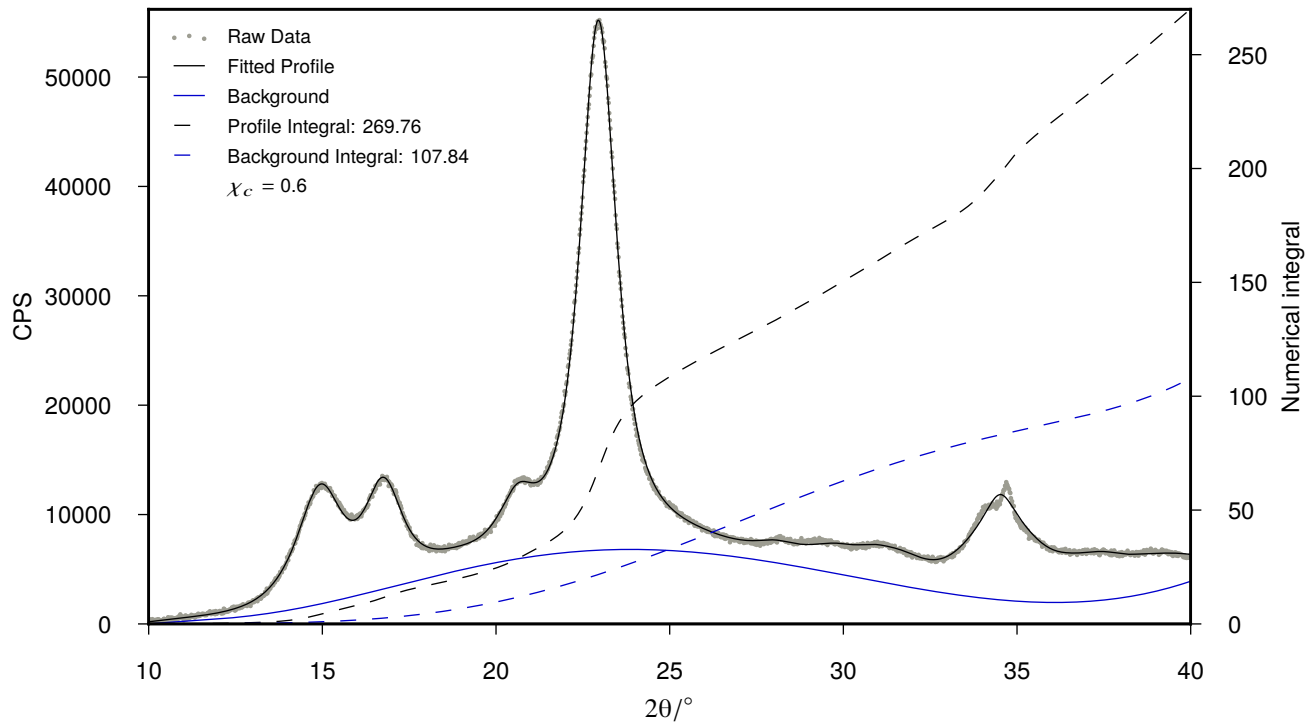

Figure S4.6. XRD of [Br][PyBnOO]-g-CNCs showing calculated profile, background, integral curves and crystallinity index

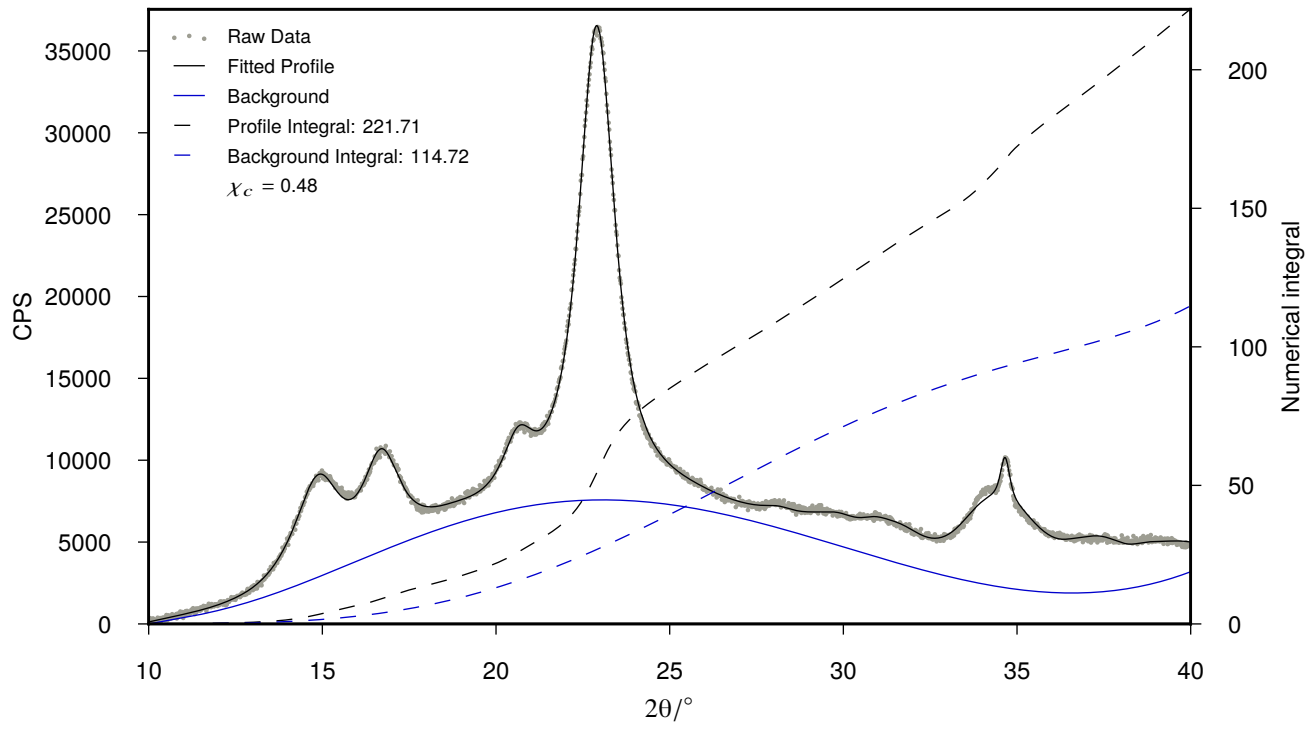

Figure S4.7. XRD of [Br][PyMeBnOO]-g-CNCs showing calculated profile, background, integral curves and crystallinity index

S5 XPS Tables

Table 1. Table of XPS data for CNCs

Orbital	**Component**	**Binding Energy /eV**	**FWHM /eV**	**Rel. A /%[a]**	**At %**
C 1s	C–C	285.00	1.02	5.81	3.45
	C–O	286.78	1.02	78.32	46.56
	O–C–O	288.34	1.02	15.87	9.43
	All			100	59.44
O 1s	C–O–H	533.03	1.26	60[b]	24.24
	O–C–O	533.63	1.26	40[b]	16.15
	All			100	40.39
S 2p[c]	S(-2) $j = 3/2$	162.33	1.60	34.51	0.06
	S(-2) $j = 1/2$	163.63	1.60	17.25	0.03
	S(VI) $j = 3/2$	168.80	1.60	32.16	0.05
	S(VI) $j = 1/2$	170.44	1.60	16.07	0.03
	All			100	0.17

[a] Area relative to other components of same orbital.
[b] Fixed to reflect stoichiometry.
[c] Rel. A/separation fixed to reflect spin-orbit splitting[6]

Table 2. Table of XPS data for [Br][PyBnOO]-g-CNCs

Orbital	Component	Binding Energy /eV	FWHM /eV	Rel. A /%[a]	At %
C 1s	C=C[b]	284.66	1.11	20.09	13.52
	C–C	285.00	1.11	8.38	5.64
	C=C*–C=O[b]	285.40	1.11	2.48	1.67
	C–O	286.07	1.11	46.18	31.07
	C-N^{+}[b]	286.52	1.11	7.52	5.06
	O–C–O	287.50	1.11	9.98	6.71
	O–C=O	288.76	1.11	3.61	2.43
	$\pi - \pi*$	292.58	2.75	1.76	1.18
	All			100	67.28
O 1s[b]	O–C=O*	530.85	1.31	4.43	1.26
	C–O–H	532.27	1.31	54.59	15.48
	O–C–O	532.87	1.31	36.56	10.37
	O*–C=O	533.88	1.31	4.42	1.25
	All			100	28.36
S 2p[c]	S(-2) $j = 3/2$	161.85	1.52	18.31	0.14
	S(-2) $j = 1/2$	163.01	1.52	9.36	0.07
	S(VI) $j = 3/2$	167.38	1.52	47.87	0.37
	S(VI) $j = 1/2$	168.54	1.52	24.46	0.19
	All			100	0.77
N 1s	N	399.37	1.12	15.56	0.28
	N^{+}	401.94	1.12	84.44	1.52
	All			100	1.80
Br 3d[c]	$j = 5/2$	67.13	0.97	59.86	0.72
	$j = 3/2$	68.17	0.97	40.14	0.48
	All			100	1.20
Cl 2p[c]	Cl- $j = 3/2$	197.08	1.55	53.97	0.31
	Cl- $j = 1/2$	198.68	1.55	26.98	0.15
	C-Cl $j = 3/2$	200.00	1.55	12.70	0.07
	C-Cl $j = 1/2$	201.60	1.55	6.35	0.04
	All			100	0.57

[a] Area relative to other components of same orbital.
[b] Rel. A fixed to reflect stoichiometry. Rel. position based on literature values.[7]
[c] Rel. A/separation fixed to reflect spin-orbit splitting[6, 8, 9]

Table 3. Table of XPS data for [Br][PyMeBnOO]-g-CNCs

Orbital	Component	Binding Energy /eV	FWHM /eV	Rel. A /%[a]	At %
C 1s	C=C[b]	284.66	1.14	33.24	24.99
	C–C	285.00	1.14	11.97	9.00
	C=C*–C=O[b]	285.40	1.14	4.11	3.09
	C–O	286.07	1.14	21.65	16.28
	C-N^{+}[b]	286.57	1.14	12.44	9.35
	O–C–O[c]	287.55	1.14	4.33	3.25
	O–C=O	288.75	1.14	5.16	3.88
	$\pi - \pi*$	292.14	3.97	7.11	5.35
	All			100	75.19
O 1s[b]	O–C=O*	530.76	1.54	11.35	2.11
	C–O–H	532.21	1.54	46.31	8.62
	O–C–O	532.81	1.54	31.01	5.77
	O*–C=O	533.50	1.54	11.35	2.11
	All			100	18.61
S 2p[d]	S(-2) $j = 3/2$	161.93	1.41	5.71	0.08
	S(-2) $j = 1/2$	163.09	1.41	2.92	0.04
	S(VI) $j = 3/2$	167.17	1.41	60.48	0.85
	S(VI) $j = 1/2$	168.33	1.41	30.90	0.44
	All			100	1.41
N 1s	N	399.13	1.15	14.22	0.37
	N^{+}	401.80	1.15	85.78	2.24
	All			100	2.61
Br 3d[d]	$j = 5/2$	66.97	0.92	59.86	0.81
	$j = 3/2$	68.01	0.92	40.14	0.54
	All			100	1.35
Cl 2p[d]	Cl- $j = 3/2$	196.71	1.41	57.29	0.48
	Cl- $j = 1/2$	198.31	1.41	28.63	0.24
	C-Cl $j = 3/2$	199.87	1.41	9.39	0.08
	C-Cl $j = 1/2$	201.47	1.41	4.69	0.04
	All			100	0.84

[a] Area relative to other components of same orbital.
[b] Rel. A fixed to reflect stoichiometry. Rel. position based on literature values.[7]
[c] Rel. A fixed to reflect stoichiometry
[d] Rel. A/separation fixed to reflect spin-orbit splitting[6, 8, 9]

S6 XPS spectra

S6.1 Wide scans

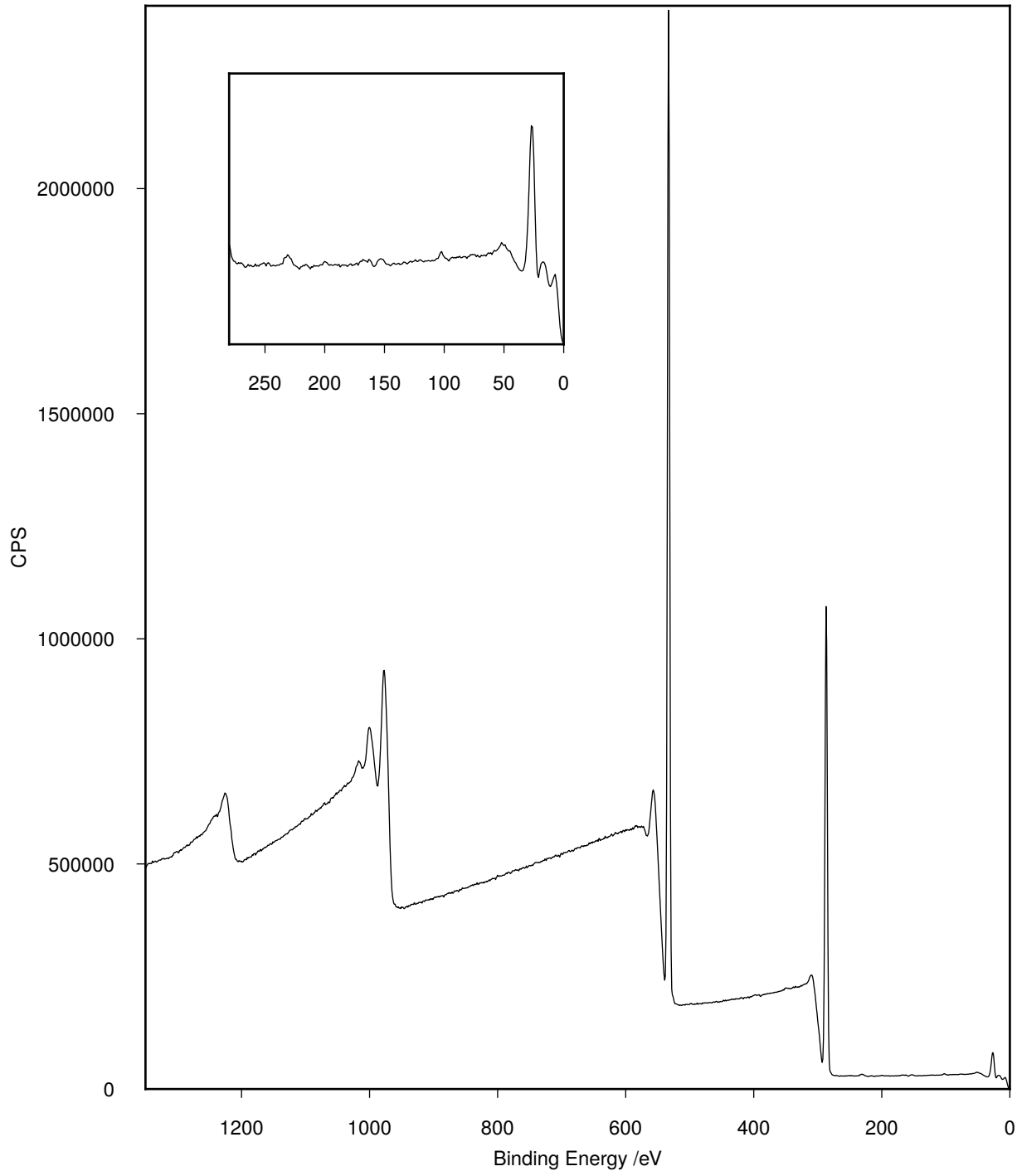

Figure S6.8. XPS wide scan of unmodified CNCs

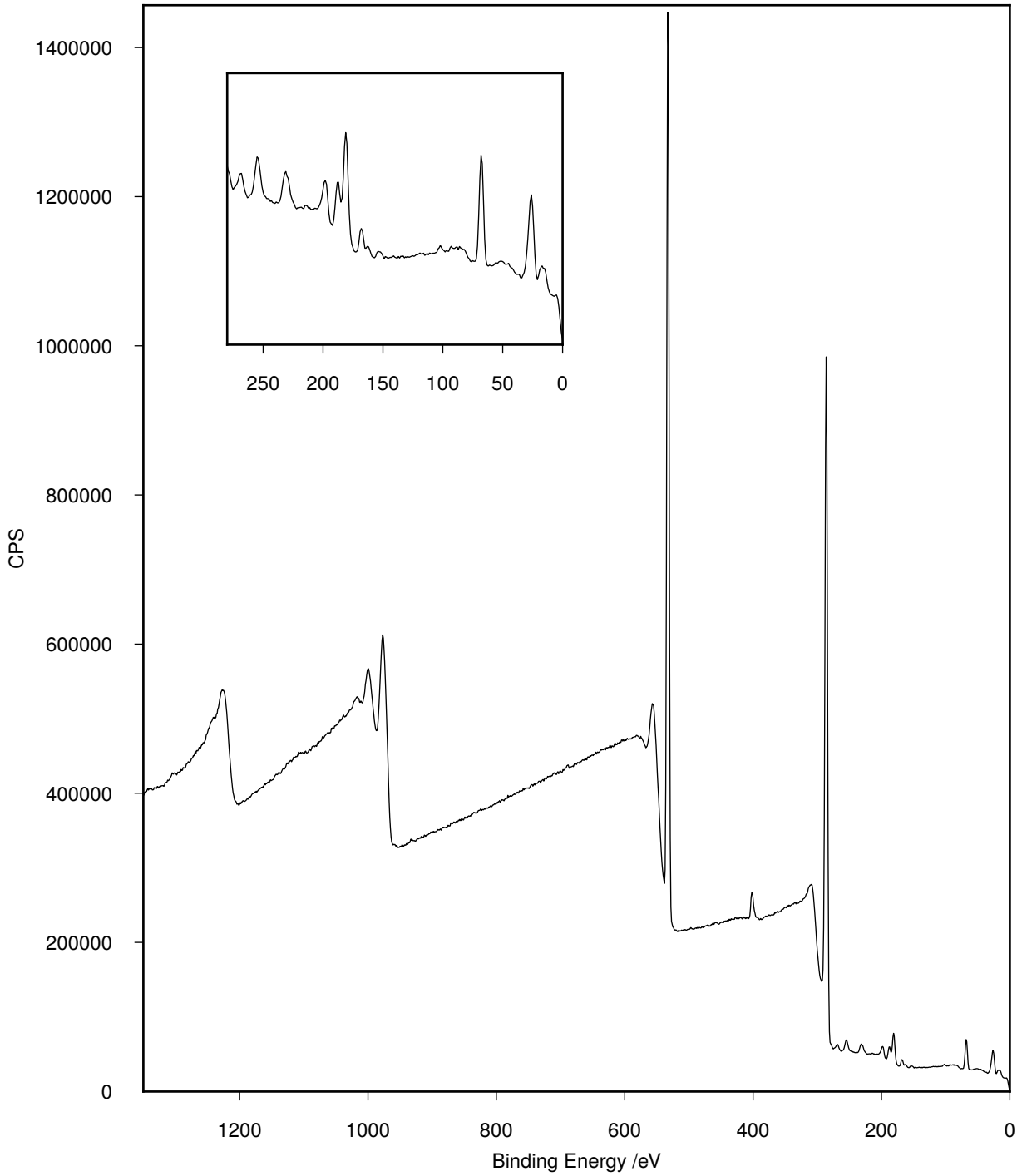

Figure S6.9. XPS wide scan of [Br][PyBnOO]-g-CNCs

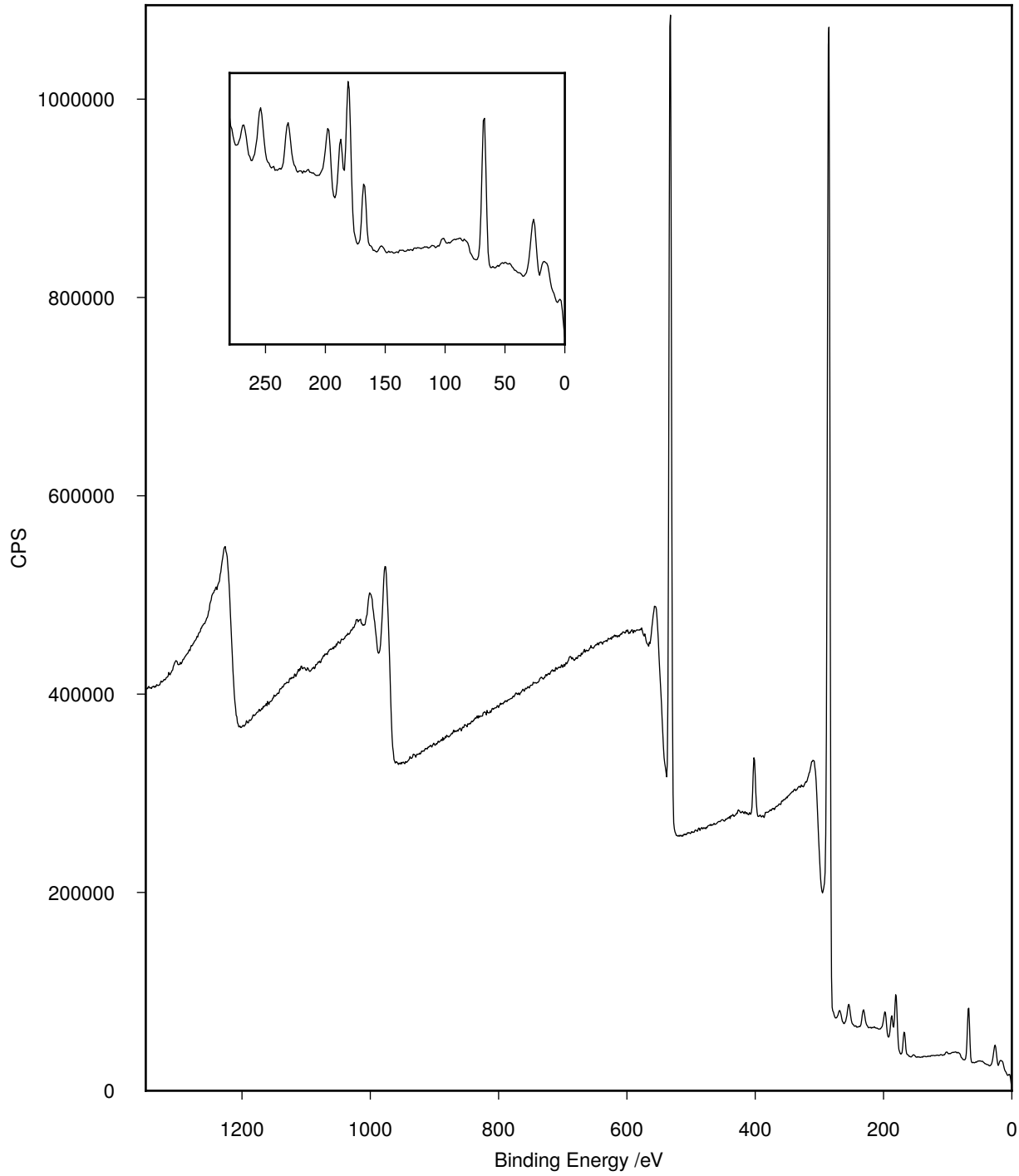

Figure S6.10. XPS wide scan of [Br][PyMeBnOO]-g-CNCs

S6.2 Carbon 1s spectra

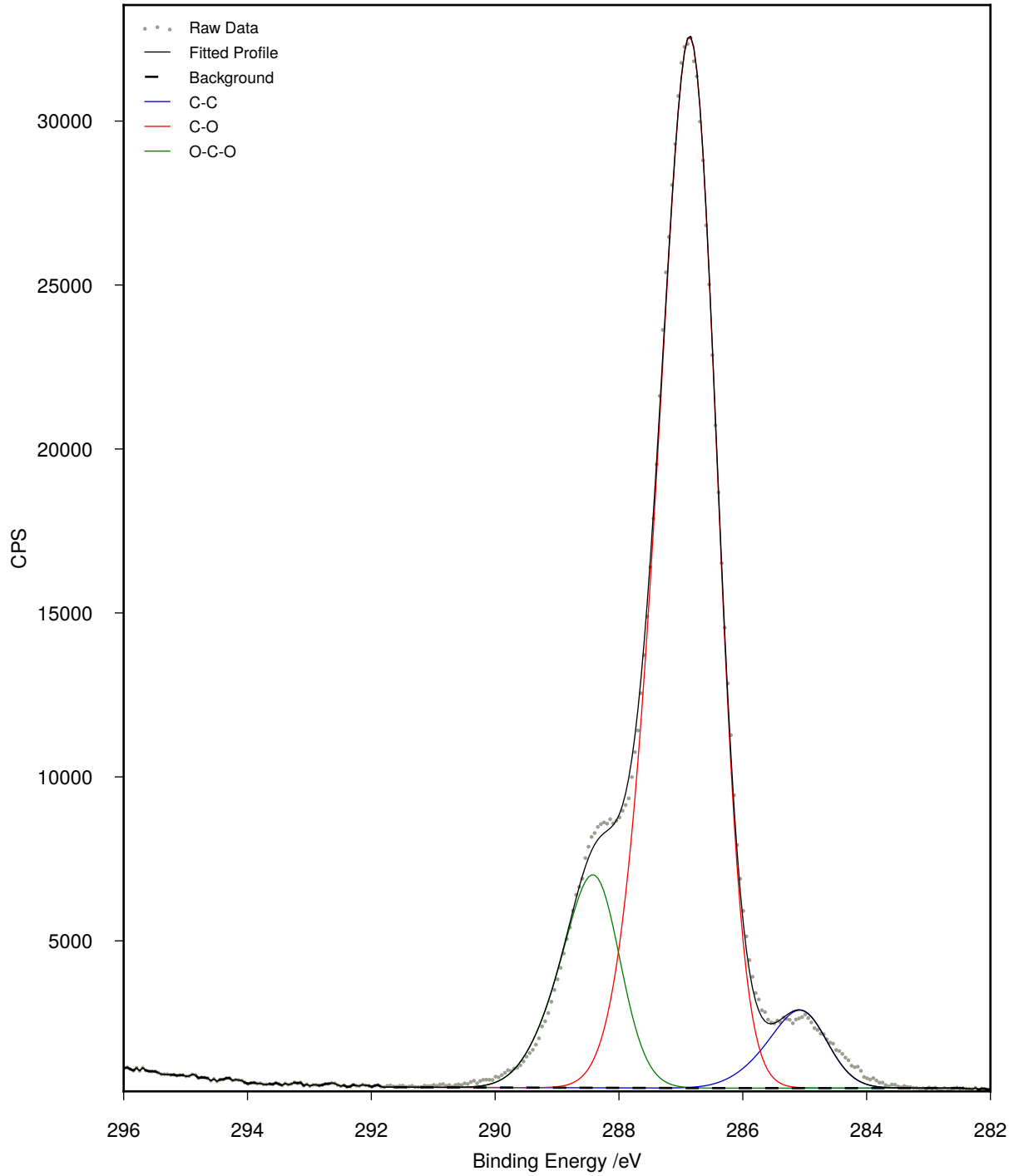

Figure S6.11. XPS carbon 1s high resolution scan of unmodified CNCs

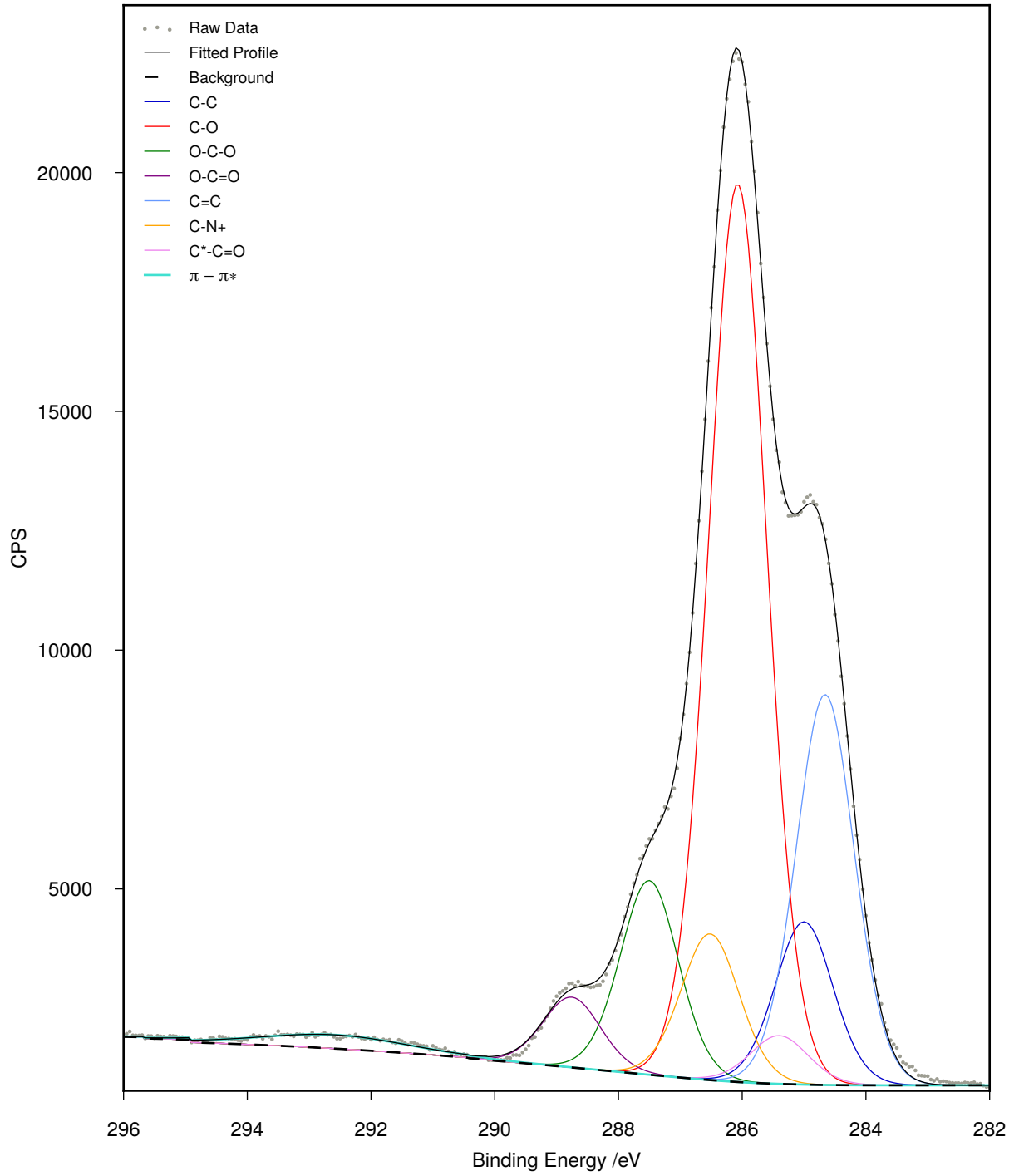

Figure S6.12. XPS carbon 1s high resolution scan of [Br][PyBnOO]-g-CNCs

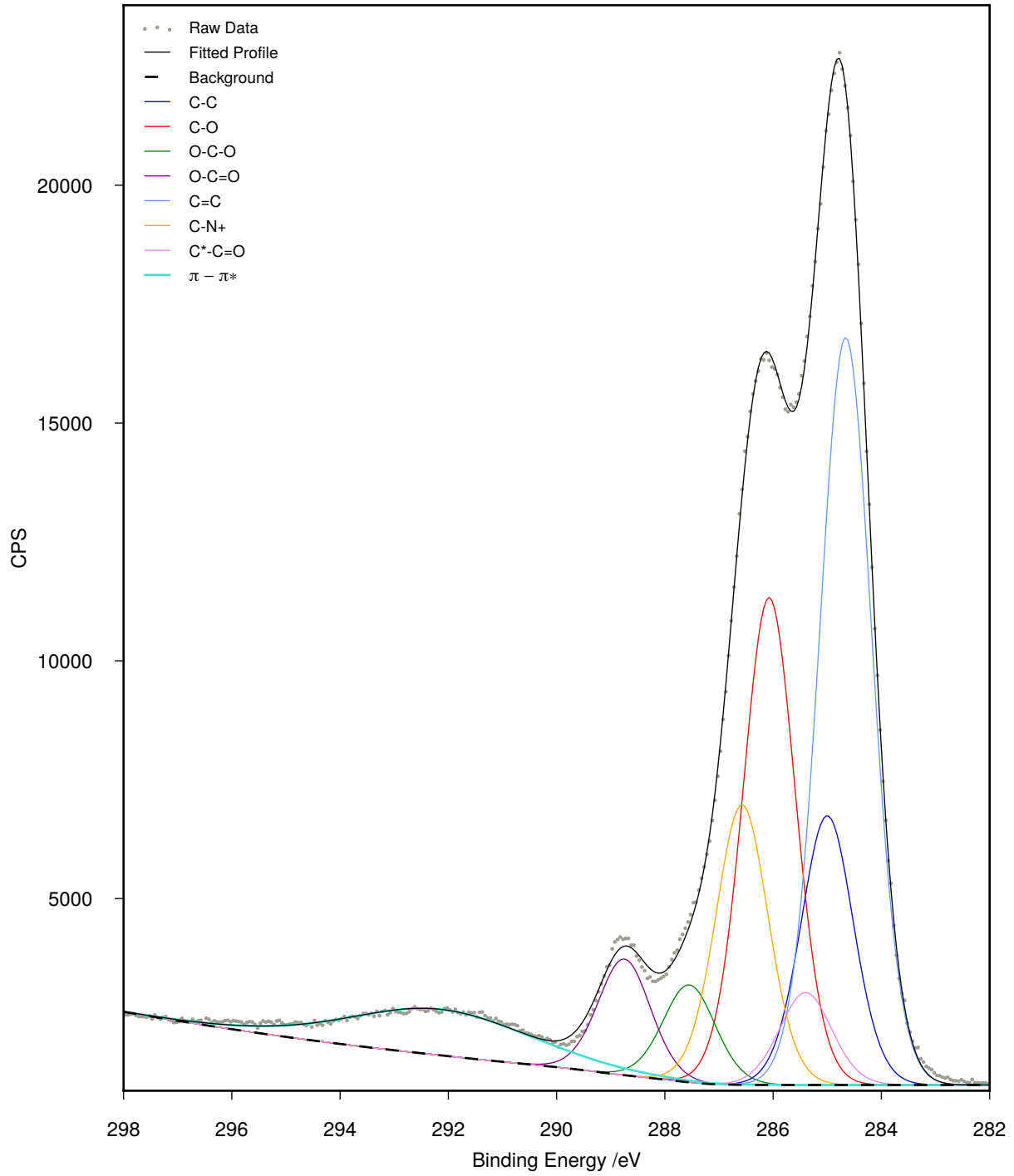

Figure S6.13. XPS carbon 1s high resolution scan of [Br][PyMeBnOO]-g-CNCs

S6.3 Oxygen 1s spectra

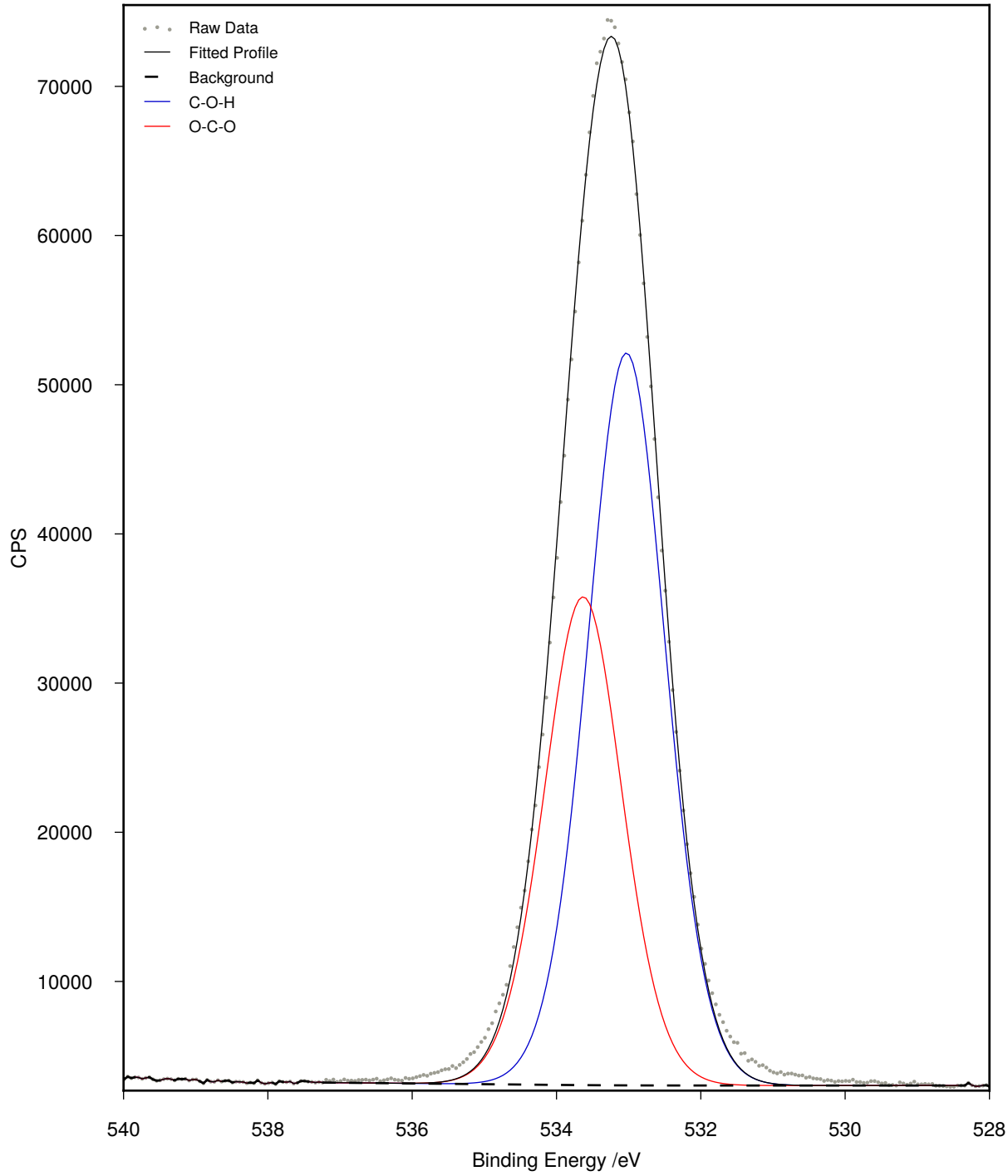

Figure S6.14. XPS oxygen 1s high resolution scan of unmodified CNCs

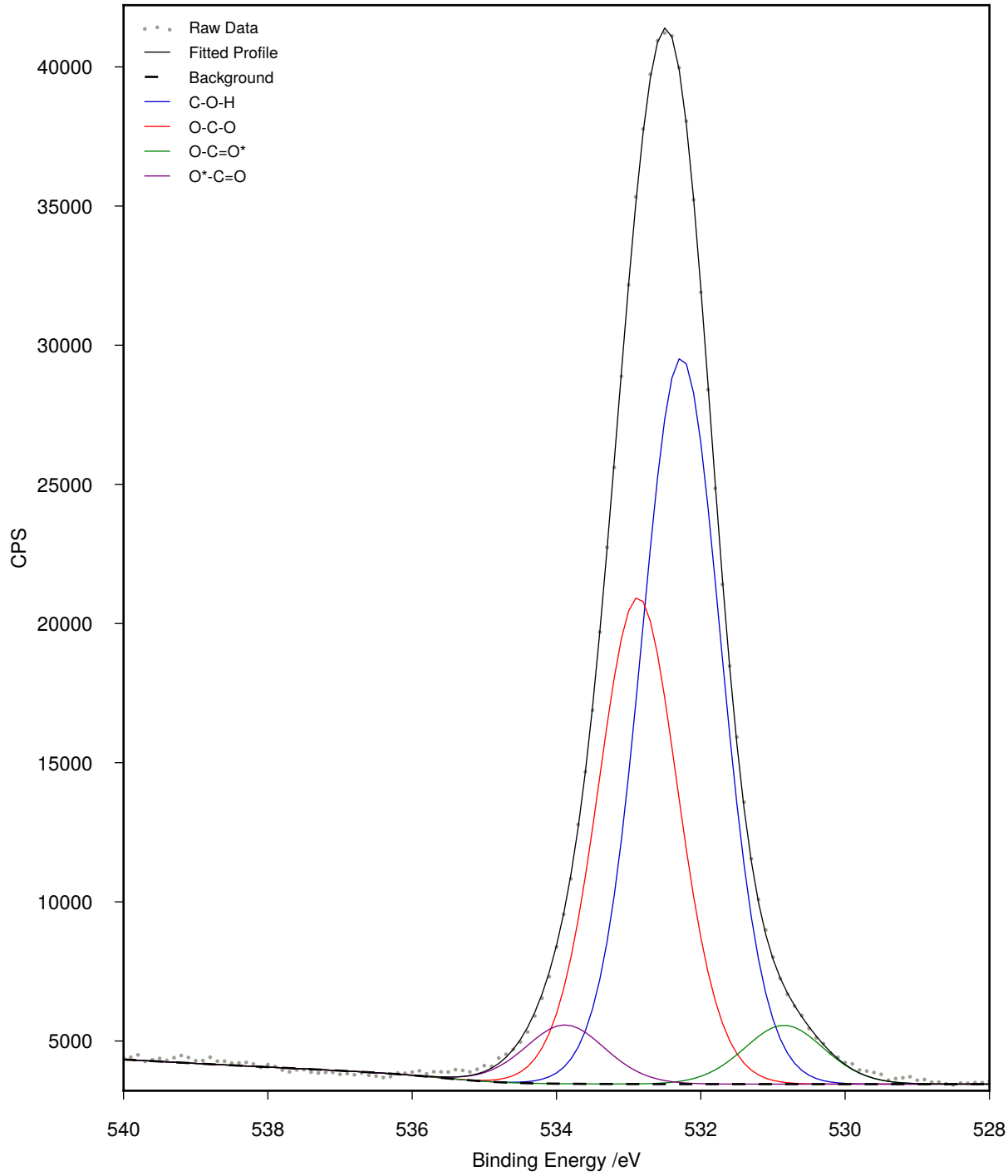

Figure S6.15. XPS oxygen 1s high resolution scan of [Br][PyBnOO]-g-CNCs

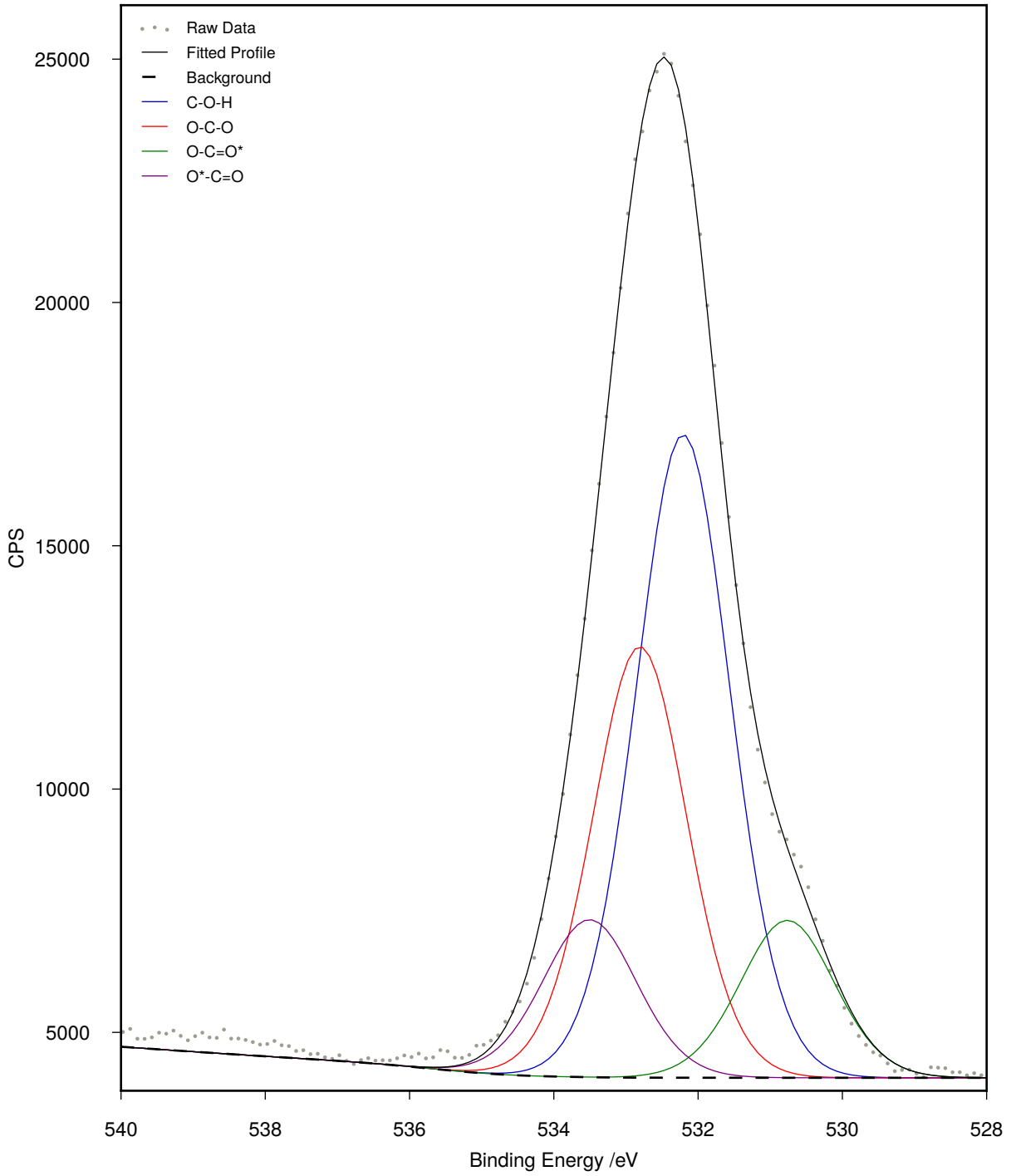

Figure S6.16. XPS oxygen 1s high resolution scan of [Br][PyMeBnOO]-g-CNCs

S6.4 Sulfur 2p spectra

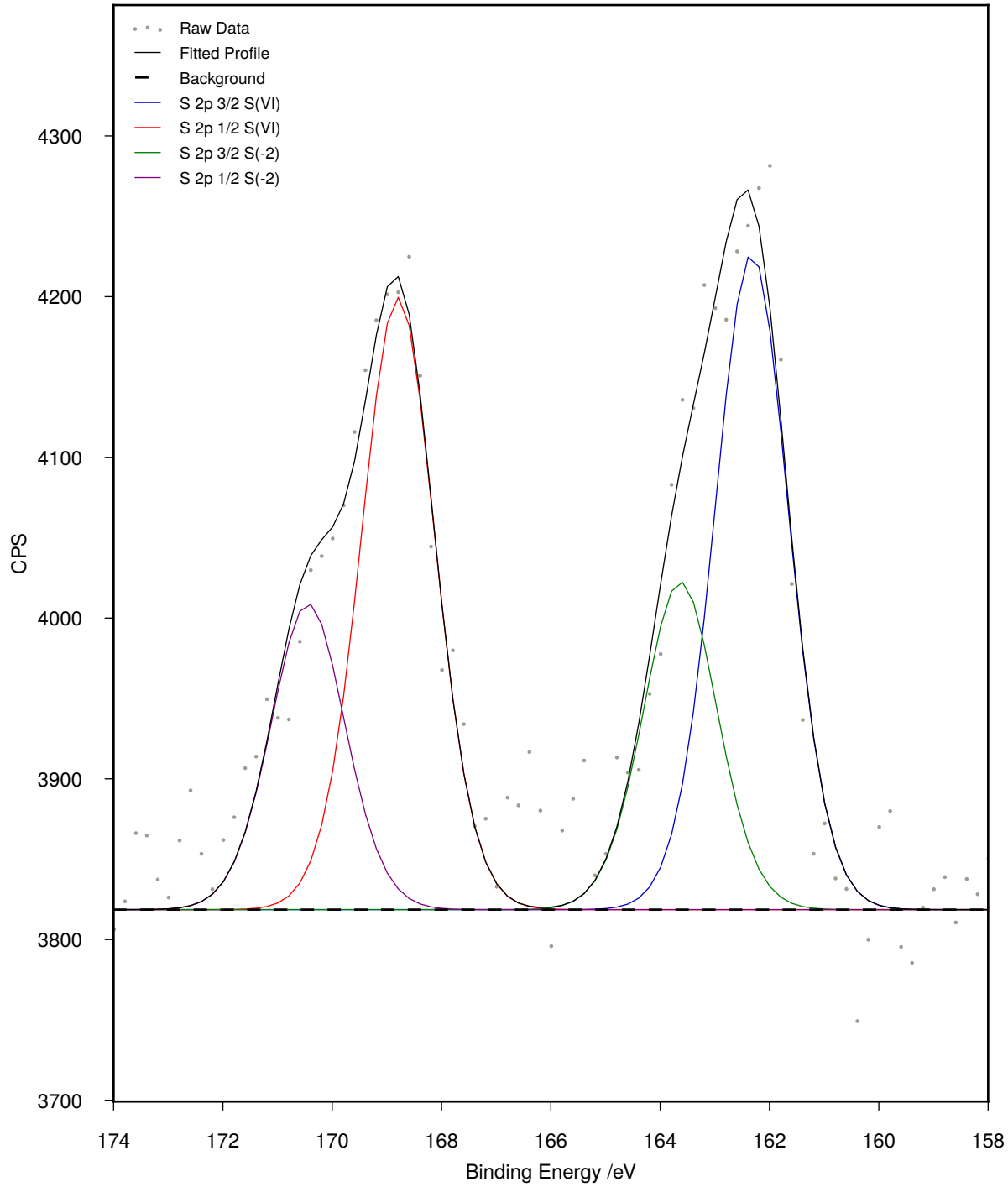

Figure S6.17. XPS sulfur 2p high resolution scan of unmodified CNCs

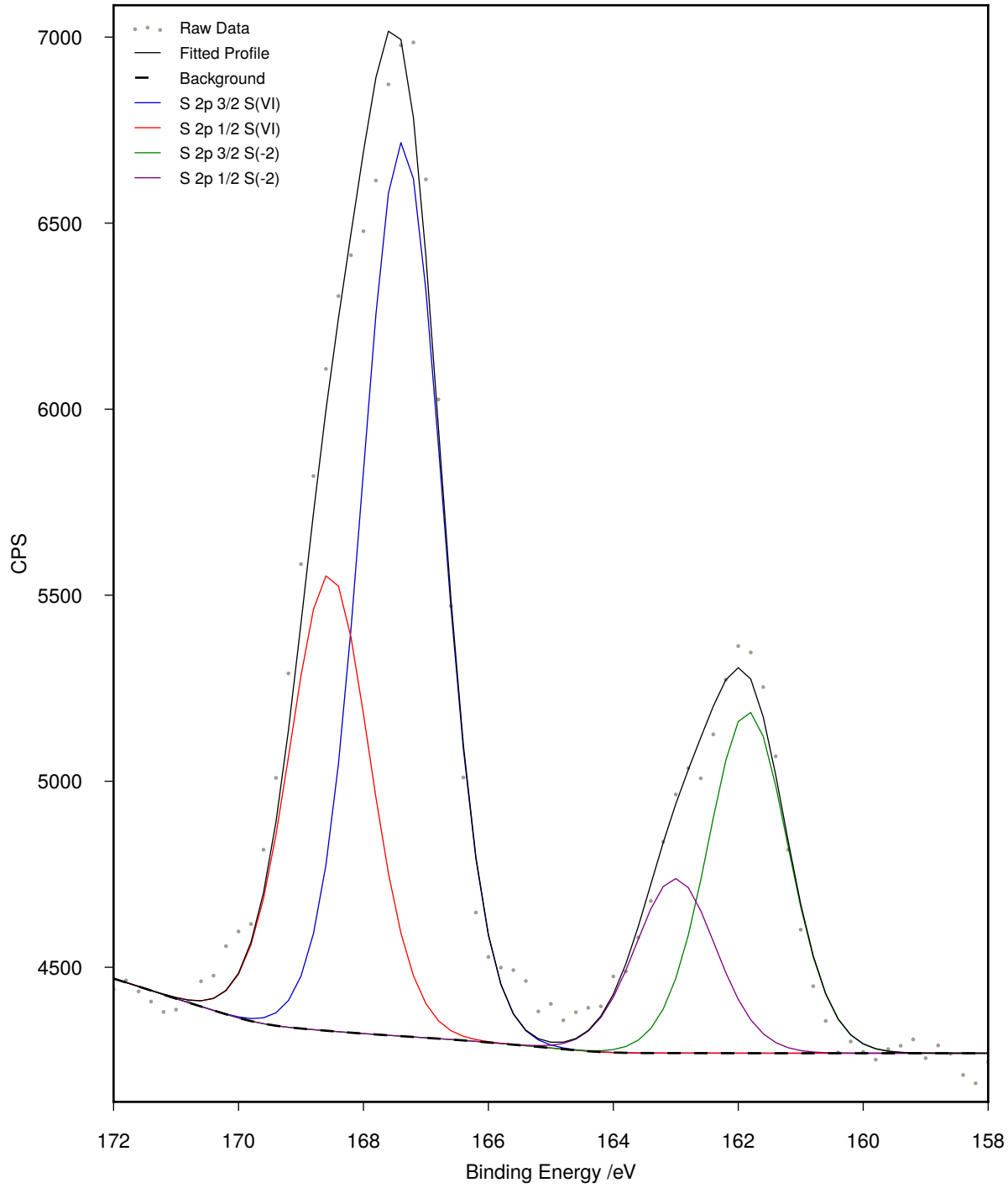

Figure S6.18. XPS sulfur 2p high resolution scan of [Br][PyBnOO]-g-CNCs

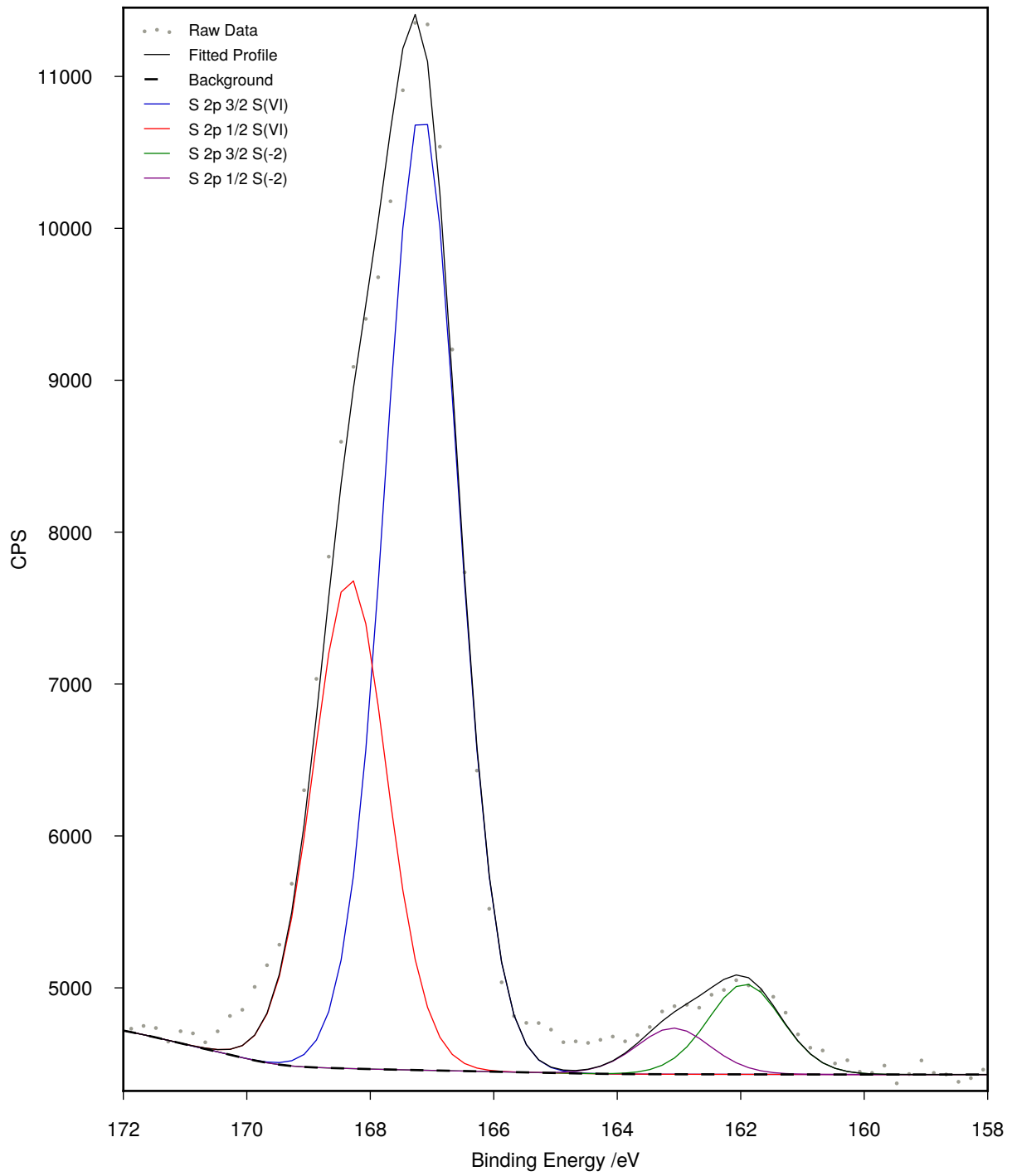

Figure S6.19. XPS sulfur 2p high resolution scan of [Br][PyMeBnOO]-g-CNCs

S6.5 Nitrogen 1s spectra

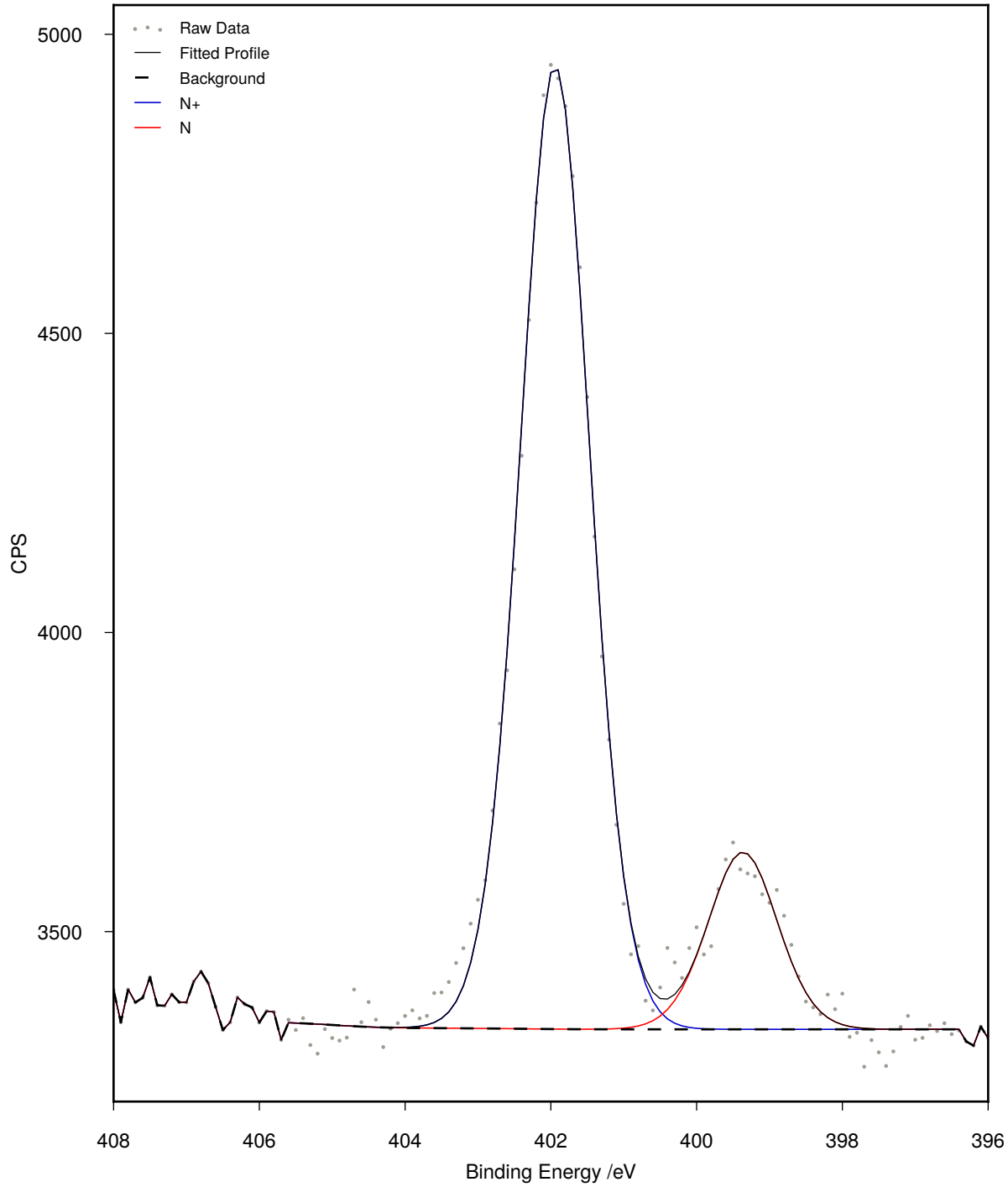

Figure S6.20. XPS nitrogen 1s high resolution scan of [Br][PyBnOO]-g-CNCs

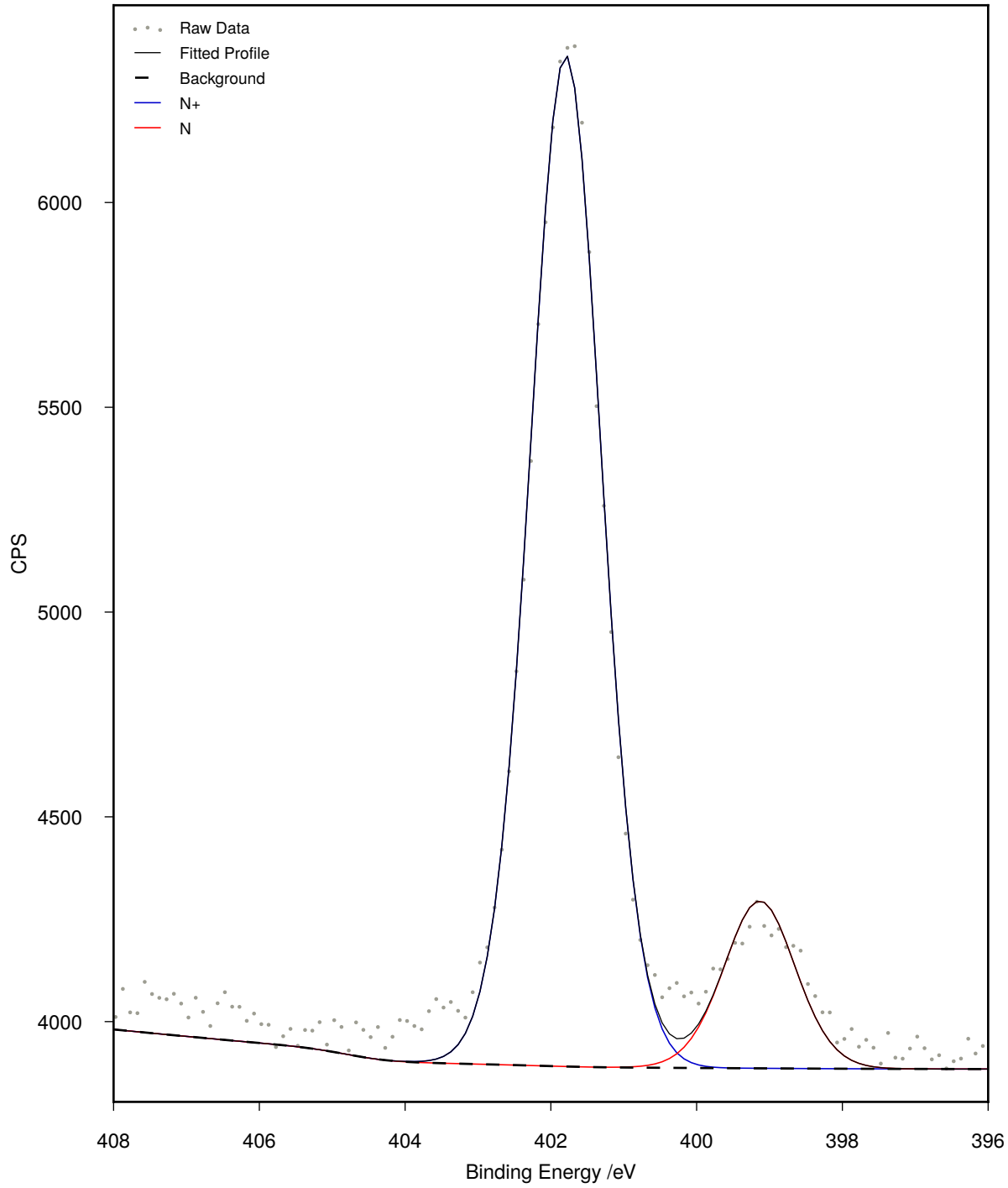

Figure S6.21. XPS nitrogen 1s high resolution scan of [Br][PyMeBnOO]-g-CNCs

S6.6 Bromine 3d spectra

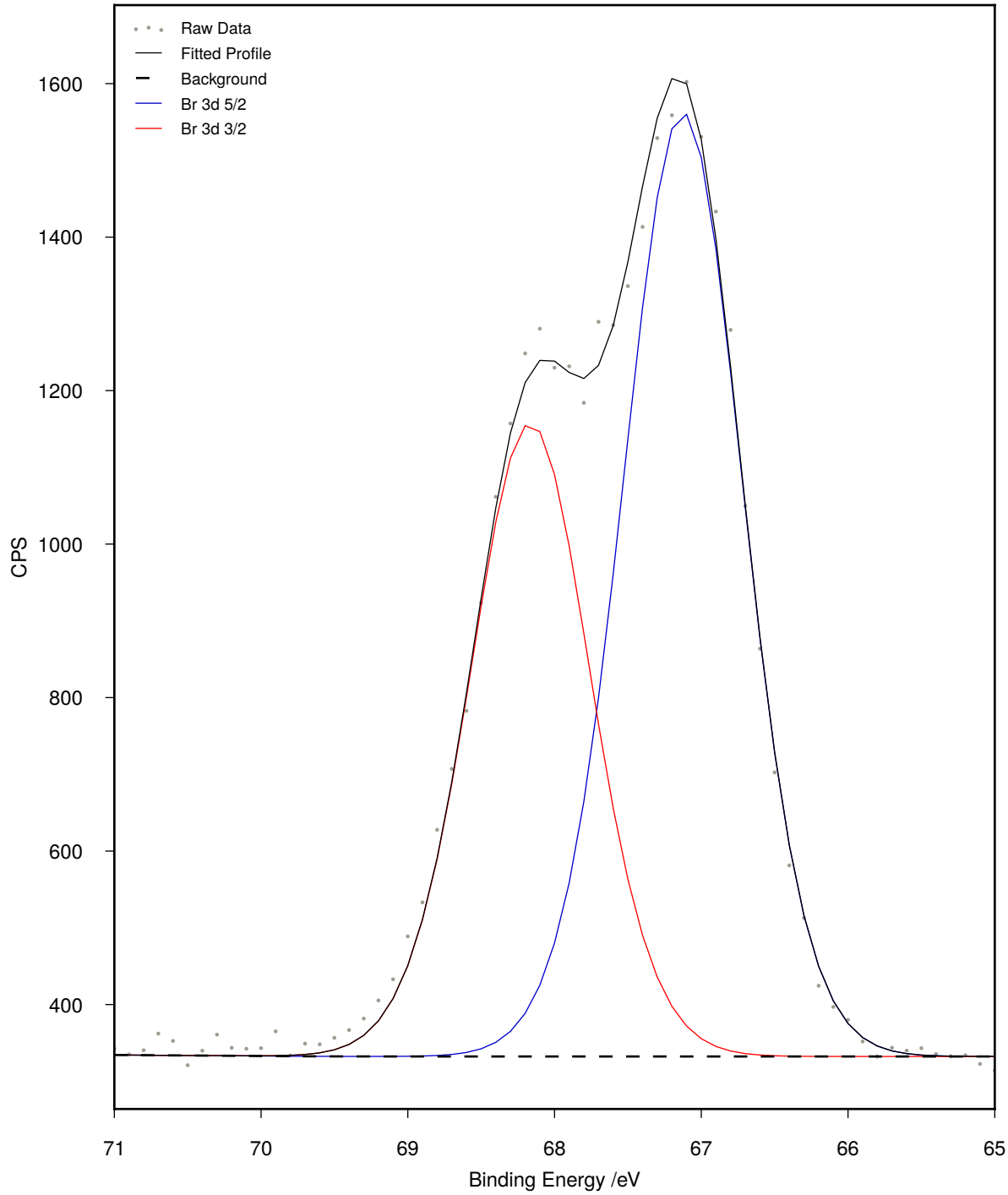

Figure S6.22. XPS bromine 3d high resolution scan of [Br][PyBnOO]-g-CNCs

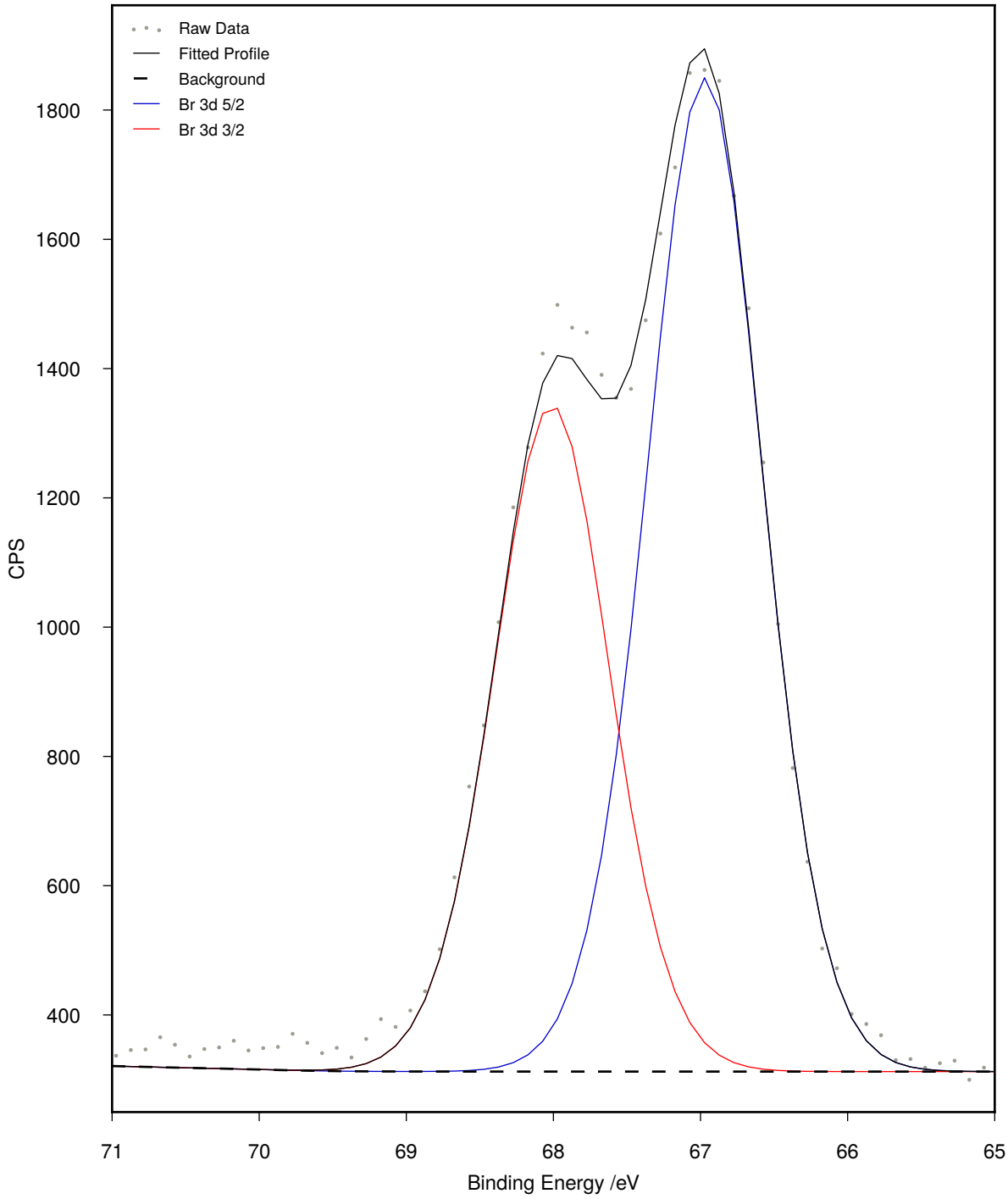

Figure S6.23. XPS bromine 3d high resolution scan of [Br][PyMeBnOO]-g-CNCs

S6.7 Chlorine 2p spectra

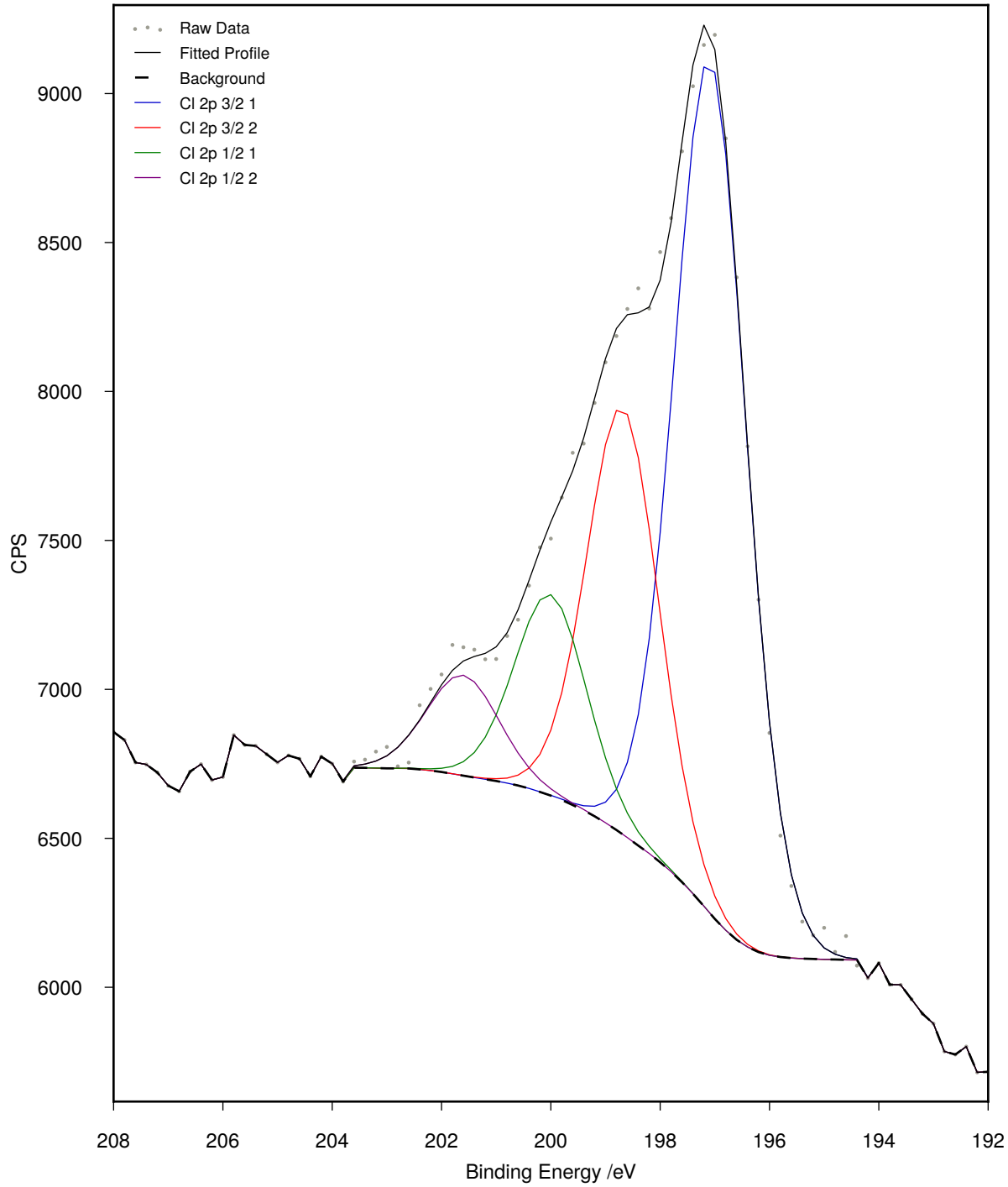

Figure S6.24. XPS chlorine 2p high resolution scan of [Br][PyBnOO]-g-CNCs

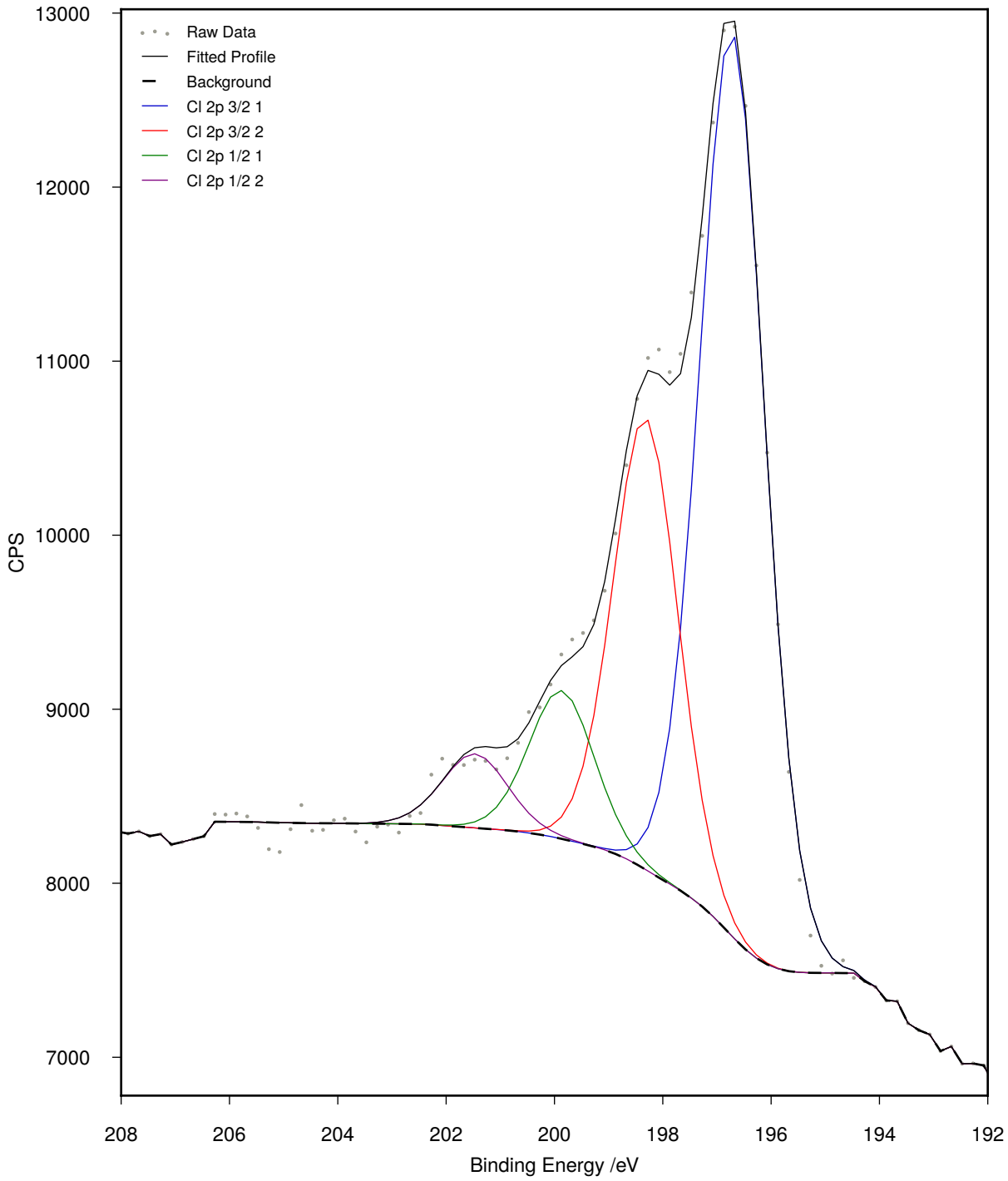

Figure S6.25. XPS chlorine 2p high resolution scan of [Br][PyMeBnOO]-g-CNCs

References

[1] Y. Maréchal, H. Chanzy, The hydrogen bond network in i_β cellulose as observed by infrared spectrometry, J. Mol. Struct. 523 (2000) 183–196.

[2] Y. Nishiyama, P. Langan, H. Chanzy, Crystal structure and hydrogen-bonding system in cellulose i_β from synchrotron x-ray and neutron fiber diffraction, J. Am. Chem. Soc. 124 (2002) 9074–9082.

[3] A. Thygesen, J. Oddershede, H. Lilholt, A. B. Thomsen, K. Ståhl, On the determination of crystallinity and cellulose content in plant fibres, Cellulose 12 (2005) 563–576.

[4] D. Briggs, J. T. Grant (Eds.), Surface Analysis by Auger and X-ray Photoelectron Spectroscopy, IM Publications, Manchester, 2003.

[5] J. Walton, P. Wincott, N. Fairley, A. Carrick, Peak Fitting with CasaXPS, Acolyte Science, Knutsford, 2010.

[6] Thermo scientific xps knowledge base - sulfur (accessed April 2015).
URL `http://xpssimplified.com/elements/sulfur.php`

[7] G. Beamson, D. Briggs (Eds.), XPS of Polymers Database, SurfaceSpectra, Manchester, 2000.

[8] Thermo scientific xps knowledge base - chlorine (accessed April 2015).
URL `http://xpssimplified.com/elements/chlorine.php`

[9] Thermo scientific xps knowledge base - bromine (accessed April 2015).
URL `http://xpssimplified.com/elements/bromine.php`